Contents lists available at ScienceDirect

European Polymer Journal

Light induced step-growth polymerization of Donor-Acceptor-Donor (DAD) type monomers based on thiophene – [1,2,5] Chalcogenazolo[3,4-f]-benzo [1,2,3] triazole – Thiophene

Kerem Kaya [a], Ecem Aydan Alkan [b], Mustafa Yasa [b], Ali Süerkan [a], Yasemin Arslan Udum [c], Levent Toppare [b,d,e,f,*], Yusuf Yagci [a,g,*]

[a] Department of Chemistry, Istanbul Technical University, Maslak, Istanbul 34469, Turkey
[b] Department of Polymer Science and Technology, Middle East Technical University, Ankara 06800, Turkey
[c] Technical Sciences Vocational School, Gazi University, Ankara 06500, Turkey
[d] Department of Chemistry, Middle East Technical University, Ankara 06800, Turkey
[e] Department of Biotechnology, Middle East Technical University, Ankara 06800, Turkey
[f] The Center for Solar Energy Research and Application (GUNAM), Middle East Technical University, Ankara 06800, Turkey
[g] Centre of Excellence for Advanced Materials Research (CEAMR) and Chemistry Dept., Faculty of Science, King Abdulaziz University, P.O. Box 80203, Jeddah 21589, Saudi Arabia

ARTICLE INFO

ABSTRACT

Two new donor-acceptor-donor(DAD) polymers type near-infrared (NIR) absorbing polymers containining thiophene as the donor and [1,2,5] chalcogenazolo [3,4-f]-benzo [1,2,3] triazole (chalcoen = S (P1a) or Se (P1b)) derivatives as the acceptor unit were designed and synthesized via light induced step-growth polymerization. The effect of different acceptor groups on the electrochemical and optical properties of the polymers was investigated. Highest occupied molecular orbital (HOMO) energy levels of the resultant black colored soluble polymers were calculated via cyclic voltammetry (CV) as −5.17 and −5.09 eV for P1a and P1b, respectively. Optical electronic band gaps were calculated as 0.81 and 0.74 eV for P1a and P1b, respectively. Lowest unoccupied molecular orbital (LUMO) energy levels were determined as −4.37 and −4.35 eV for P1a and P1b, respectively. NMR and gel-permeation chromatography (GPC) results supported the formation of high-molecular weight species. Synthesized polymers have promising features for application in various optoelectronic devices.

1. Introduction

Since the discovery of the electrical conductivity of polyacetylene in 1977 [1], research on the synthesis of conjugated polymers (CPs) has been drastically increased [2-4]. Solution-based processability of these organic polymers allow materials to be coated using straightforward techniques like spin casting [5], dip coating [6], ink jet [7] or screen printing [8]. Consequently, especially in the last two decades, CPs have found wide applications in various technological devices such as organic field effect transistors (OFETs) [9], organic light-emitting diodes (OLEDs) [10], solar cells [4], electrochromic devices [11], photovoltaics [12], electronic displays [13], supercapacitors [14], batteries [15], sensors [16] and in many other areas [17-19].

It is the energy difference between the highest occupied molecular orbital (HOMO) and lowest unoccupied molecular orbital (LUMO), namely, the band gap that dictates the chemical and physical properties, thus the optoelectronic and electrochromic properties of the CPs [20]. A narrow band gap is essential for CPs. Since the discovery of donor-acceptor (DA) concept by Havinga, et al. in 1992 [21], numerous design approaches have been proposed. Donor-acceptor–donor (DAD) approach have become the most efficient method [22] since fine tuning of the HOMO and LUMO levels of CPs can be achieved by the selection of appropriate D and A units inducing an intramolecular charge-transfer (ICT) which results in very low band gap [23]. DAD type CPs are expected to possess a significantly reduced the band gap (<2 eV), an enhanced charge separation and mobility making them perfect candidates for many of the above mentioned devices [24]. Moreover, DAD type CPs absorb light at NIR region which is crucial for photovoltaic

---
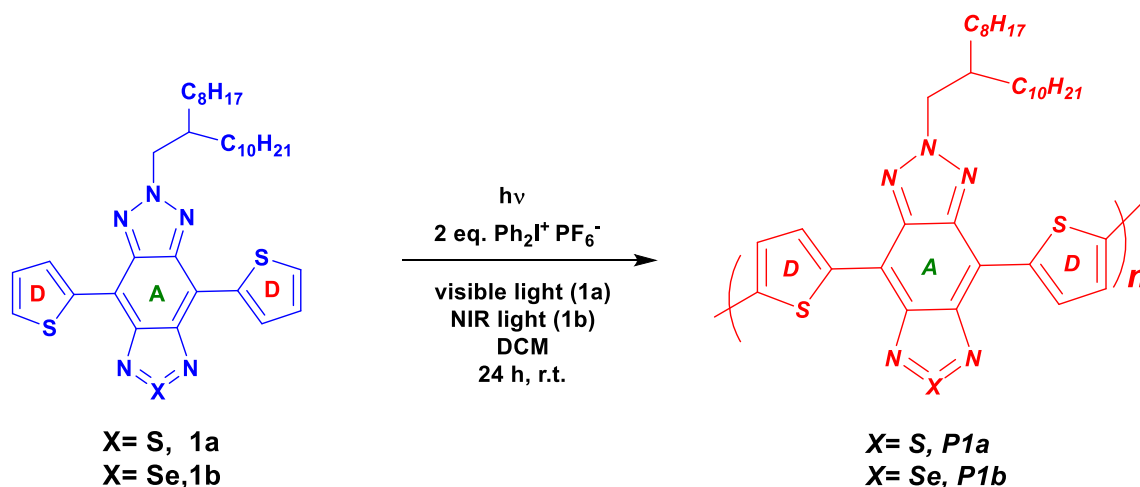
Scheme 1. Overall reaction scheme for the light induced polymerization of 1a and 1b.

devices [25].

A great variety of D and A units are available for the design of DAD type CPs. Thiophene, furan, pyrrole, carbazole and several other heterocyclic compounds have been extensively used as D units in the production of DAD type CPs. However, among these heterocycles, thiophene is by far the most widely used unit since CPs based on thiophene have good thermal stability, strong and broad absorption and narrow band gap suitable for many optoelectronic applications [26]. Concerning the A unit, benzo(chalcogen)diazole [27], benzotriazole [28], benzoquinoxaline [29,30] and similar compounds have been effectively used for the purpose [31,32]. Electron withdrawing strength of benzo(chalcogen)diazole unit can be further increased by fusion of triazole unit to the vacant sites of the phenyl ring. This highly electron-deficient planar backbone when combined with electron-rich thiophene units can generate DAD type CPs with desired properties. Selenium heteroatom is much larger than sulfur atom making the CPs more effective in extending the absorption spectrum toward NIR region [33]. Fully conjugated rigid planar structures with strong π - π interactions have poor solubility in most of the organic solvents. Another advantage of the incorporation of triazole unit is the possible functionalization of the nitrogen atom with long alkyl chains which significantly increase both solubility and molecular weight of the final polymer [34].

Generally, DAD type CPs have been synthesized using chemical or electrochemical polymerization techniques [35–37]. Chemical polymerization techniques are mostly based on cross-coupling reactions having major disadvantages such as the requirement of highly inert atmosphere, high temperature and the use of expensive transition metal catalysts (Pd or Ni) [38]. Another disadvantage of the cross-coupling reactions is the trace amount of halogen or transition metal left after the reaction which negatively affect the optoelectronic properties of the final polymer [32]. Electrochemical polymerization, compared with the chemical polymerization, produces polymers in a more controlled fashion without using metal catalysts which results in the formation of polymers with less defects and less side products. However, electrochemical polymerization requires sophisticated setups and can produce limited amount of polymers due to the formation of polymers only on the electrodes. Another drawback of the electrochemical polymerization is the decrease of the reaction rate during polymerization due to the formation of polymer on the electrode [39].

In response to the world's rapidly increasing need for renewable energy, polymerization reactions induced by light have become very important for achieving sustainable chemistry [40]. Light induced reactions occur at room temperature, require small amount or no solvent, have higher efficiency than conventional methods. Moreover, spatiotemporal control which is crucial for modern electronic device production can be realized through light induced polymerization method [41]. Many different photoinitiating systems for free radical and cationic polymerization acting at broad range wavelength of electromagnetic spectrum have been reported [42-47]. However, the corresponding step-growth polymerization has been scarcely investigated. In our group, we reported several light induced step-growth polymerizations of conjugated monomers such as thiophene [48], *2*,5-dithiophenyl (thieno[3,4-b] thiophene) derivatives [49,50], *N*-ethylcarbazole [51,52], pyrene [53] and 4,4′- bis(N-carbazolyl)-1,1′-biphenyl [54].

In light of the previous study on photosensitized radical and cationic polymerizations, [55] herein, we report light induced step-growth polymerization of thiophene substituted [1,2,5] chalcogenazolo[3,4-f]-benzo [1,2,3] triazole (chalcogen = S (1a), Se (1b)) using diphenyl iodonium salt under visible and NIR light irradiation, respectively (Scheme 1).

To the best of our knowledge, this is first example of DAD type polymer synthesis by photopolymerization technique. The polymerization is believed to proceed through photoinduced electron transfer reactions (PET) as previously shown for thiophene and carbazole derivatives [48,51]. Electrochemical, spectral and spectroelectrochemical characterizations of the obtained polymers were investigated. The effect of chalcogen on electrochemical and optical properties was also examined.

2. Experimental

2.1. Materials

The conjugated monomers 1a and 1b were synthesized according to previously reported procedure [27]. Diphenyliodonium hexafluorophosphate (DPI) > 98% was purchased from Sigma-Aldrich and was used without further purification. All the solvents were purified according to conventional purification methods prior to use.

2.2. Photopolymerization procedure

A Philips 150 Watts PAR38E E27 halogen pressed glass type bulb with strong visible and IR-A (NIR) emission (Fig. S1) was used for the photopolymerization reactions. The light intensity inside the reaction tube was calculated to be ~200 mW.cm^{-2}. The light bulb was attached to the top of a photoreactor setup equipped with a large air cooling fan. 250 mg of DPI (~0.6 mmol) and 180 mg of 1a or 200 mg of 1b (~0.3 mmol) were dissolved in 1 mL of dichloromethane (DCM) and were transferred inside a 20 mL Schlenk tube which was previously heated, degassed and flushed with nitrogen for three times. After 24 h of

Table 1
Light induced step-growth polymerization results of 1a and 1b.

Monomer [a]	Conversion [b] (%)	M_n [c] (kg/mol)	$Đ$ [c]
1a	69	3.68	1.76
1b	84	6.90	1.35

[a] Reaction conditions: 1 mL dichloromethane solvent with monomer: DPI (1:2/ mol:mol) ratio.
[b] Conversions were determined gravimetrically.
[c] Molecular weight averages (M_n) and dispersity ($Đ$) indices were determined by GPC.

irradiation inside the photoreactor, the dark colored polymers were precipitated into methanol. After filtration and washing with hot methanol to remove the unreacted monomers, the polymers were kept at least 24 h inside a vacuum-oven at 50 °C in order to avoid any solvent impurities.

2.3. Instrumentation

Polymers were characterized using Gel Permeation Chromatography (GPC), Nuclear Magnetic Resonance (NMR) and ultraviolet-visible light (UV–vis). Molecular weight measurements were conducted on a TOSOH EcoGPC system equipped with an auto sampler system, a temperature controlled pump, a column oven, a refractive index (RI) detector, a purge and degasser unit, and TSK gel superhZ2000 column with 4. 6 mm ID × 2 cm column dimensions. Tetrahydrofuran (THF) was used as the eluent at flow rate of 1.0 mL.min^{-1} at 40 °C. RI detector was calibrated with polystyrene standards having very narrow molecular-weight distributions. GPC data were analyzed using Eco-GPC Analysis software. Number average molecular weight (M_n) and dispersity indices ($Đ$) were determined using GPC with polystyrene standards having very narrow molecular weight distribution. UV–visible spectra were recorded with a JASCO V-770 Spectrophotometer. ^{1}H NMR (500 MHz) spectra were recorded in deuterated chloroform with tetramethylsilane as an internal standard on Agilent VNMRS500 spectrometer at 25 °C. The electrochemical properties of the polymers P1a and P1b were investigated via cyclic voltammetry (CV) in a solution of 0.1 M Bu$_4$NPF$_6$/ACN electrolyte/solvent couple at a scan rate of 100 mV/s. CV studies were performed in a three-electrode cell system using an ITO-coated glass as the working electrode and platinum and silver wires as the counter and reference electrodes, respectively.

3. Results and discussion

3.1. Characterization of the polymers

1a and 1b were readily polymerized in dichloromethane solvent upon irradiation at visible and NIR light in the presence of DPI, respectively. The blue and green colored solutions of 1a and 1b turned to black after 24 h irradiation. (Fig. S2). After precipitation, drying and dedoping procedures, the resulting polymers were analyzed using GPC. The results obtained are tabulated in Table 1. GPC traces of the polymers were presented in the supporting information (Fig. S3).

^{1}H NMR spectra of the polymers (P1a-P1b) exhibited clear broadening in the aromatic and aliphatic regions with respect to the corresponding monomers indicating the formation of polymeric species. (Fig. 1a-b).

In this connection, it should be pointed out that photosensitization activity of both 1a and 1b was more efficient in the cationic polymerization as cationic species formed rapidly react with the monomers. In the step-growth polymerization, 1b has yielded polymers with higher efficiency and molecular weight due to the higher absorption in the NIR region.

3.2. Proposed mechanism

Since 1a and 1b absorb the light at the irradiated wavelength region where DPI is transparent (Fig. S4), a plausible mechanism for the light induced step-growth polymerization involves first the absorption and formation of exciplex between photoexcited monomers and DPI. Then PET reaction within the exciplex yields radical cations of 1a and 1b which were previously proved by laser flash photolysis studies [42]. Successive proton release and radical coupling reactions essentially yield P1a and P1b as depicted in Scheme 2. It should be noted that in this mechanism, the ground state charge transfer complex formation is excluded since the absorption of the monomers does shift to longer wavelengths with the addition of DPI.

3.3. Electrochemical characterization

Redox behavior of the polymers was investigated by cyclic voltammetry (CV). Polymers were dissolved in chloroform and spray coated on indium tin oxide coated glass substrates as thin films. A three-electrode system was used to conduct CV investigations. ITO was used as the working electrode, a platinum wire as the counter electrode and a silver wire as reference electrode. Single scan cyclic voltammograms of P1a
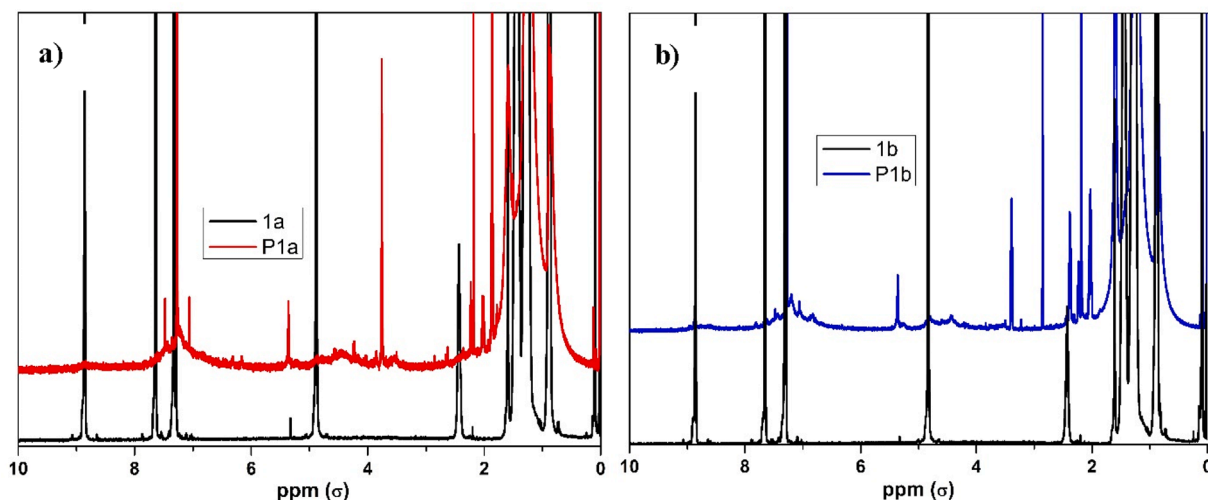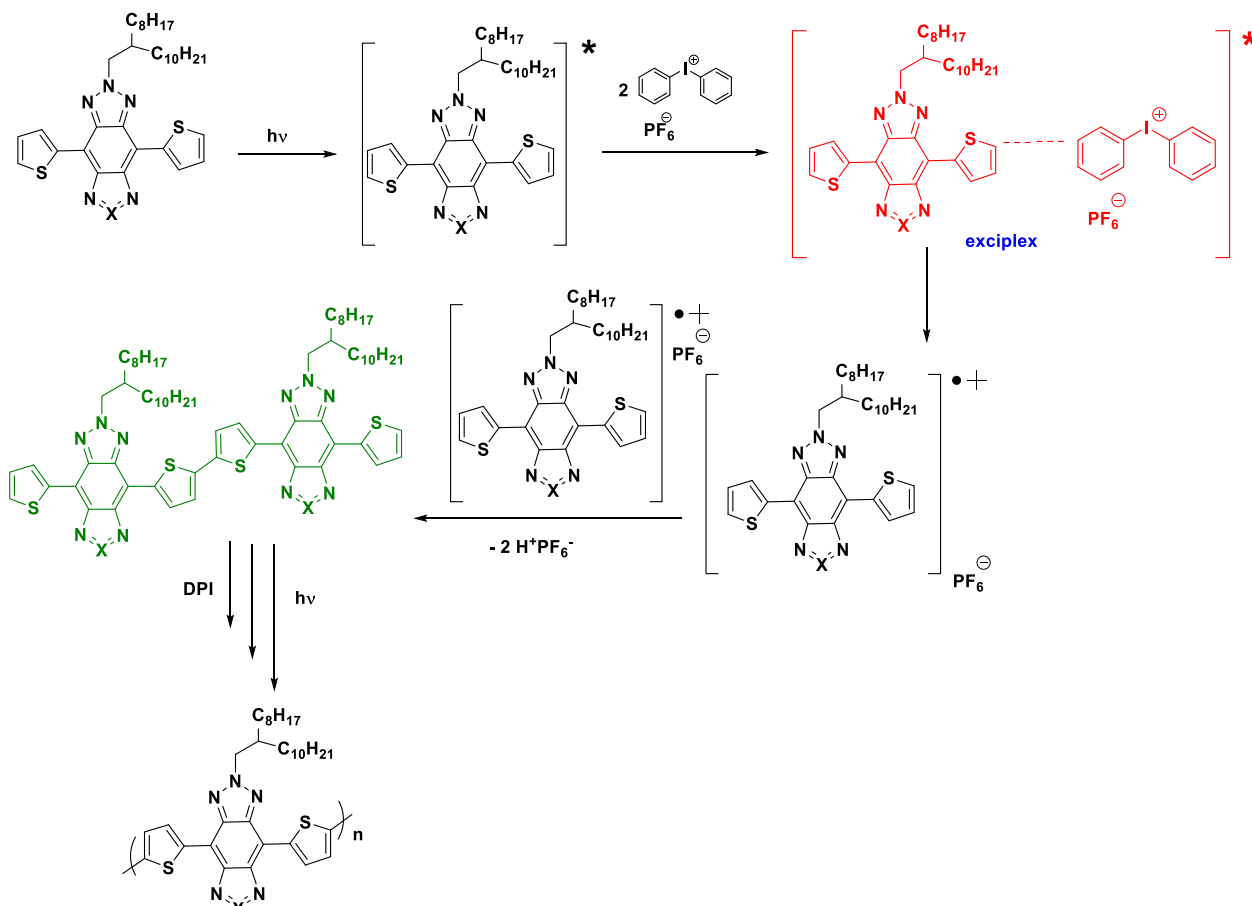

Fig. 1. ^{1}H NMR spectra of (a) 1a-P1a (b) 1b-P1b in CDCl$_3$ solvent (500 MHz).

Scheme 2. Reaction mechanism for the light induced step-growth polymerization of 1a and 1b.
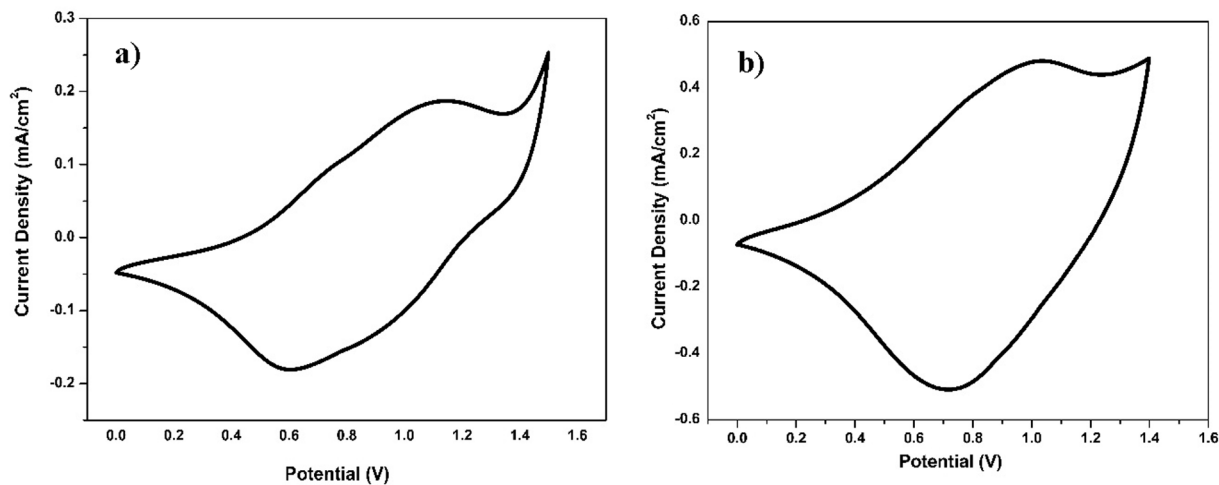

Fig. 2. Cyclic voltammograms of (a) P1a and (b) P1b in 0.1 M Bu$_4$NPF$_6$/ACN solution.

Table 2
The energy levels of P1a and P1b.

	E$_{p-doping}$(V)	E$_{p-dedoping}$(V)	E$^{ox}_{onset}$(V)	HOMO(eV)	LUMO(eV)	λ$_{max}$ (nm)	λ$_{onset}$ (nm)	E$_g^{op}$(eV)
P1a	1.14	0.60	0.42	−5.17	−4.37	690	1540	0.81
P1b	1.03	0.72	0.34	−5.09	−4.35	975	1685	0.74

*LUMO energy levels were calculated by subtracting the optical band gap values from HOMO levels.
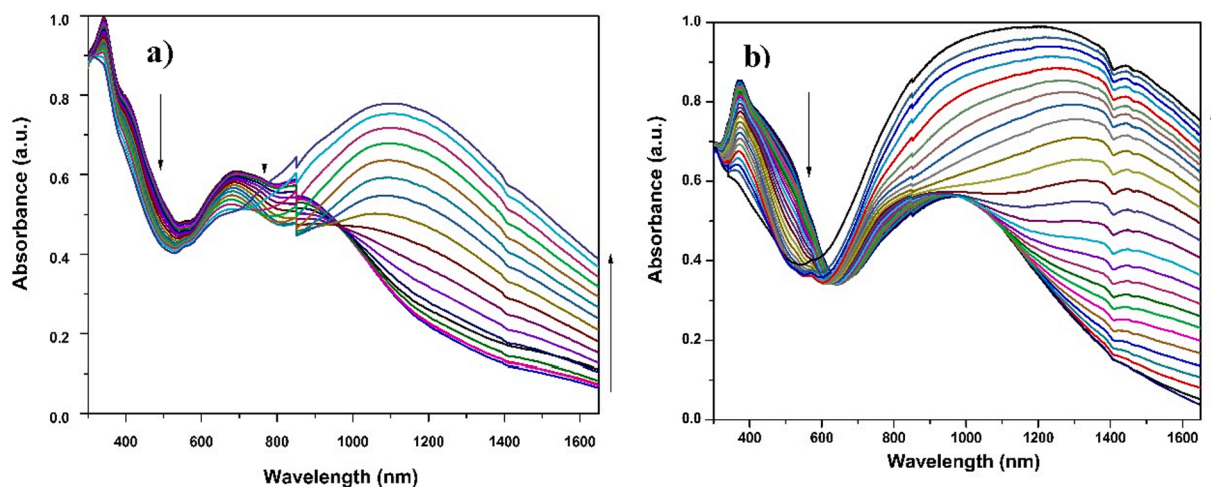
Fig. 3. Electronic absorption spectra of (a) P1a and (b) P1b in 0.1 M Bu$_4$NPF$_6$/ACN solution.

and P1b are illustrated in Fig. 2.

As reported in Table 2, P1b exhibited lower oxidation potential at 1.03 V compared to that of P1a at 1.14 V. This can be attributed to the electron-rich character of selenophene units in the P1b polymer backbone.

HOMO and LUMO energy levels were calculated by using CV results using following equations;

$$E_{HOMO}(eV) = -\left(4.75 + E_{oxidation,onset}\right)$$

$$E_{LUMO}(eV) = -\left(4.75 + E_{reduction,onset}\right)$$

HOMO energy levels of P1a and P1b were estimated to be −5.17 eV and −5.09 eV, respectively. As the polymers have solely p-character, LUMO energy levels of copolymers were calculated from the difference of optical band gap and HOMO energy levels (Table 2).
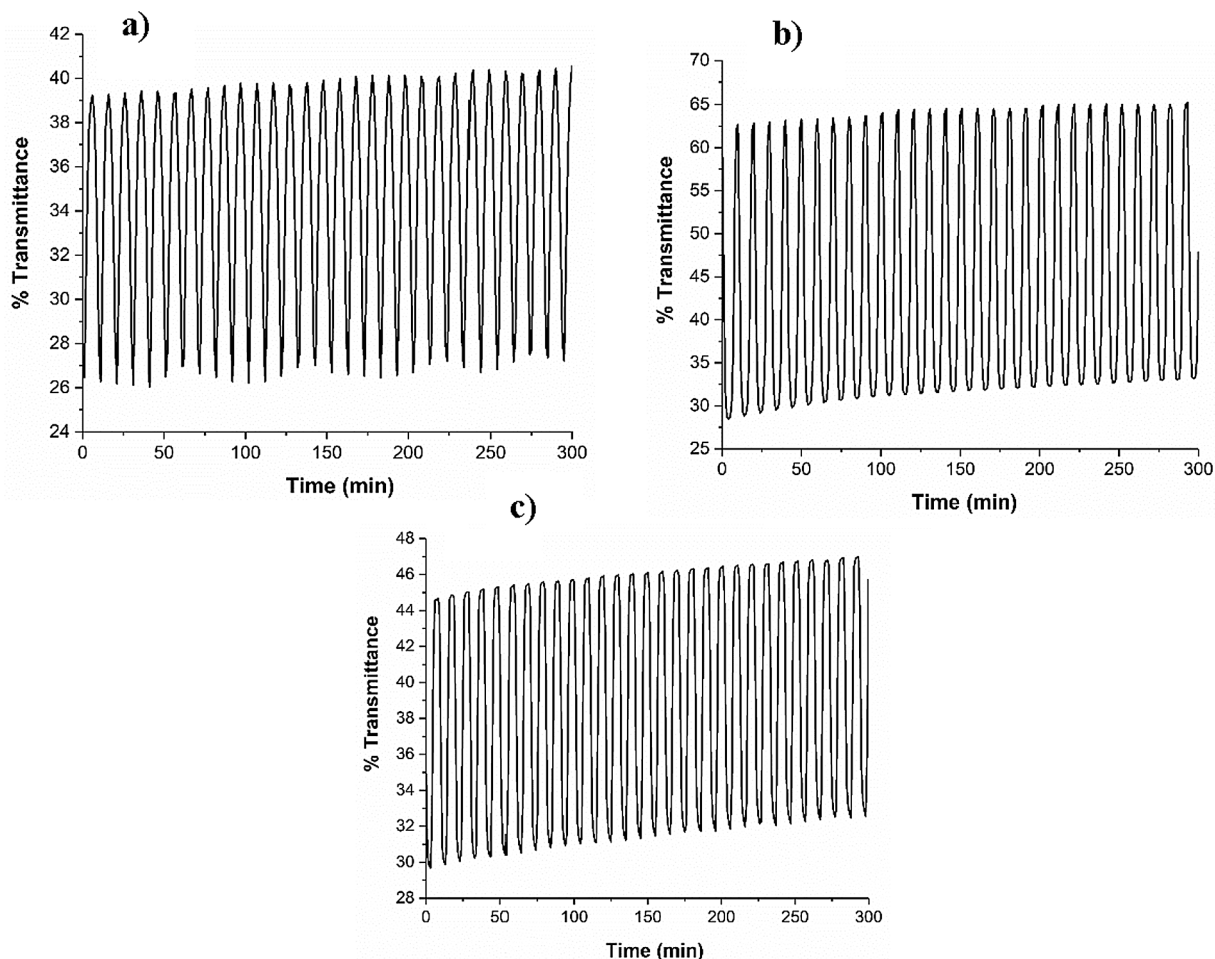

Fig. 4. Percent transmittance changes of P1b in 0.1 M Bu$_4$NPF$_6$/ACN solution at a) 480 nm b) 975 nm c) 1300 nm.

Table 3
Optical properties of P1b.

Polymer	λ (nm)	Optical Contrast (ΔT %)	Switching Time (s)
P1b	480	14	3.0
	975	15	1.8
	1300	34	1.9

3.4. Spectroelectrochemical characterization

Spectroelectrochemical studies were conducted to investigate the electronic and optical properties of the polymers. Polymers were dissolved in chloroform and spray coated on ITO-coated glass substrate to form polymer films. The absorption spectra of the polymer films were displayed in 0.1 M Bu$_4$NPF$_6$/ACN solution in order to analyze the response of the polymers to the doping process. (see Fig. 3) Absorption is monitored by increasing the applied potential incrementally between 0.00 and 1.30 V for P1a and P1b. The changes in the absorption spectra are shown (see Fig. 3).

The reduced polymers show a maximum absorbance at 345 nm/690 nm for P1a, 375 nm/975 nm for P1b related to the interband π-π* transitions of the aromatic form of neutral polymers. When the oxidation starts, new polaronic and bipolaronic levels are generated. In the fully oxidized state the polymers still absorbed in the NIR region, resulting with an absorption in almost whole range above 500 nm up to 1600 nm. The optical band gaps of P1a and P1b were calculated as 0.81 eV and 0.74 eV, respectively. As observed in the electrochemical results, Se increases the electron density in the polymer chain due to the stronger electron donating ability compared to the S atom. As a result, it is possible to obtain a red shift in neutral state absorption and a lower band gap for Se containing P1b (Table 2).

3.5. Kinetic Analysis

Optical contrasts and switching times of polymers were determined by conducting kinetic studies. These were performed using polymer films coated on ITO coated glass electrodes, in a solution of 0.1 M of Bu$_4$NPF$_6$/ACN. Changes in the percent transmittance were recorded at specific wavelengths determined from the absorption spectra (see Fig. 4). Percent transmittance changes were monitored under applied potentials. The transmittance values continuously change between fully neutral and oxidized states within time intervals of 5 s. The switching times of the P1b were calculated from percent transmittance change as the time necessary for the color-changing process at a 95% contrast value. Percent transmittance changes of P1b were calculated as 14 % at 480 nm; 15 % at 975 nm; and 34 % at 1300 nm. Corresponding switching times are also illustrated in Table 3.

4. Conclusions

Novel DAD type CPs comprising thiophene donor unit and long alkyl substituted [1,2,5]chalcogenazolo[3,4-f]-benzo[1,2,3]triazole acceptor unit were designed and synthesized using light induced step-growth polymerization. Electrochemical, spectroelectrochemical and kinetic characterizations of the resultant black polymers were performed. Spectroelectrochemical characterizations revealed extremely narrow optical band gaps, for P1a and P1b as 0.81 and 0.74 eV, respectively. Se increases the electron density in the P1b structure due to the stronger electron donating ability compared to that of S. As a result, it is possible to obtain a red shift in neutral state absorption and a lower band gap for Se containing P1b. Moreover, Se has a larger contribution to LUMO level due to its higher polarizability. It is concluded that Se containing polymer has a lower band gap, higher optical absorbance, thus is a better candidate as DAD type polymer for electrochromic devices. This study opened a new pathway for the synthesis of DAD type CPs using a facile strategy and without the need for expensive transition metal catalysts or sophisticated electrochemical setups.

CRediT authorship contribution statement

Kerem Kaya: Investigation, Visualization, Data curation. **Ecem Aydan Alkan:** Investigation, Data curation. **Mustafa Yasa:** Formal analysis. **Ali Süerkan:** Data curation, Visualization. **Yasemin Arslan Udum:** Data curation, Investigation. **Levent Toppare:** Conceptualization. **Yusuf Yagci:** Conceptualization, Supervision.

Declaration of Competing Interest

The authors declare that they have no known competing financial interests or personal relationships that could have appeared to influence the work reported in this paper.

Appendix A. Supplementary material

Supplementary data to this article can be found online at https://doi.org/10.1016/j.eurpolymj.2021.110831.

References

[1] C.K. Chiang, C.R. Fincher, Y.W. Park, A.J. Heeger, H. Shirakawa, E.J. Louis, S.C. Gau, A.G. MacDiarmid, Electrical Conductivity in Doped Polyacetylene, Phys. Rev. Lett. 39 (17) (1977) 1098–1101.

[2] B.J. Schwartz, Conjugated Polymers as Molecular Materials: How Chain Conformation and Film Morphology Influence Energy Transfer and Interchain Interactions, Annu. Rev. Phys. Chem. 54 (1) (2003) 141–172.

[3] A. Facchetti, π-Conjugated Polymers for Organic Electronics and Photovoltaic Cell Applications, Chem. Mater. 23 (3) (2011) 733–758.

[4] Y.-J. Cheng, S.-H. Yang, C.-S. Hsu, Synthesis of Conjugated Polymers for Organic Solar Cell Applications, Chem. Rev. 109 (11) (2009) 5868–5923.

[5] J. Jaczewska, A. Budkowski, A. Bernasik, I. Raptis, E. Moons, D. Goustouridis, J. Haberko, J. Rysz, Ordering domains of spin cast blends of conjugated and dielectric polymers on surfaces patterned by soft- and photo-lithography, Soft Matter 5 (1) (2009) 234–241.

[6] G.W. Kim, E.H. Kwon, M. Kim, Y.D. Park, Uniform and Reliable Dip-Coated Conjugated Polymers for Organic Transistors as Obtained by Solvent Vapor Annealing, J. Phys. Chem. C 123 (37) (2019) 23255–23263.

[7] B.-J. de Gans, P.C. Duineveld, U.S. Schubert, Inkjet Printing of Polymers: State of the Art and Future Developments, Adv. Mater. 16 (3) (2004) 203–213.

[8] M. Jørgensen, O. Hagemann, J. Alstrup, F.C. Krebs, Thermo-cleavable solvents for printing conjugated polymers: Application in polymer solar cells, Sol. Energy Mater. Sol. Cells 93 (4) (2009) 413–421.

[9] J. Yang, Z. Zhao, S. Wang, Y. Guo, Y. Liu, Insight into High-Performance Conjugated Polymers for Organic Field-Effect Transistors, Chem 4 (12) (2018) 2748–2785.

[10] C. Zhao, Z. Chen, R. Shi, X. Yang, T. Zhang, Recent Advances in Conjugated Polymers for Visible-Light-Driven Water Splitting, Adv. Mater. 32 (28) (2020) 1907296, https://doi.org/10.1002/adma.v32.2810.1002/adma.201907296.

[11] W.T. Neo, Q. Ye, S.-J. Chua, J. Xu, Conjugated polymer-based electrochromics: materials, device fabrication and application prospects, J. Mater. Chem. C 4 (31) (2016) 7364–7376.

[12] X. Zhan, D. Zhu, Conjugated polymers for high-efficiency organic photovoltaics, Polym. Chem. 1 (4) (2010) 409–419.

[13] S. Ahmad, Organic semiconductors for device applications: current trends and future prospects, J. Polym. Eng. 34 (4) (2014) 279–338.

[14] X. Wu, B. Huang, R. Lv, Q. Wang, Y. Wang, Highly flexible and low capacitance loss supercapacitor electrode based on hybridizing decentralized conjugated polymer chains with MXene, Chem. Eng. J. 378 (2019), 122246.

[15] J.F. Mike, J.L. Lutkenhaus, Recent advances in conjugated polymer energy storage, J. Polym. Sci., Part B: Polym. Phys. 51 (7) (2013) 468–480.

[16] M.d. Rahman, P. Kumar, D.-S. Park, Y.-B. Shim, Electrochemical Sensors Based on Organic Conjugated Polymers, Sensors 8 (1) (2008) 118–141.

[17] J. Li, J. Liu, C.-W. Wei, B. Liu, M. O'Donnell, X. Gao, Emerging applications of conjugated polymers in molecular imaging, Phys. Chem. Chem. Phys. 15 (40) (2013) 17006–17015.

[18] N. Li, Y. Dai, Y. Li, S. Dai, J. Strzalka, Q.i. Su, N. De Oliveira, Q. Zhang, P.B.J. St. Onge, S. Rondeau-Gagné, Y. Wang, X. Gu, J. Xu, S. Wang, A universal and facile

approach for building multifunctional conjugated polymers for human-integrated electronics, Matter 4 (9) (2021) 3015–3029.

[19] J. Liu, X. Xu, J. Wang, R. Sang, Z. Zhang, J. Chen, X. Lu, Q. Wang, Q. Fan, A diketopyrrolopyrrole-based conjugated polymer for efficient photodynamic and photothermal combination therapy under single 808 nm laser irradiation, Dyes Pigm. 196 (2021), 109762.

[20] Y. Xia, X. Deng, Li. Wang, X. Li, X. Zhu, Y. Cao, An Extremely Narrow-Band-Gap Conjugated Polymer with Heterocyclic Backbone and its Use in Optoelectronic Devices, Macromol. Rapid Commun. 27 (15) (2006) 1260–1264.

[21] E.E. Havinga, W. ten Hoeve, H. Wynberg, A new class of small band gap organic polymer conductors, Polym. Bull. 29 (1-2) (1992) 119–126.

[22] E. Bundgaard, F. Krebs, Low band gap polymers for organic photovoltaics, Sol. Energy Mater. Sol. Cells 91 (11) (2007) 954–985.

[23] K. Colladet, S. Fourier, T.J. Cleij, L. Lutsen, J. Gelan, D. Vanderzande, L.e. Huong Nguyen, H. Neugebauer, S. Sariciftci, A. Aguirre, G. Janssen, E. Goovaerts, Low Band Gap Donor–Acceptor Conjugated Polymers toward Organic Solar Cells Applications, Macromolecules 40 (1) (2007) 65–72.

[24] A. Singh, R. Singh, C.-M. Lin, M.K. Pola, C.-K. Chang, K.-H. Wei, H.-C. Lin, Novel fluoride-substituted donor/acceptor polymers containing benzodithiophene and quinoxaline units for use in low–band gap solar cells, Eur. Polym. J. 82 (2016) 334–346.

[25] C. Qin, Y. Fu, C.-H. Chui, C.-W. Kan, Z. Xie, L. Wang, W.-Y. Wong, Tuning the Donor-Acceptor Strength of Low-Bandgap Platinum-Acetylide Polymers for Near-Infrared Photovoltaic Applications, Macromol. Rapid Commun. 32 (18) (2011) 1472–1477.

[26] R.D. McCullough, The Chemistry of Conducting Polythiophenes, Adv. Mater. 10 (2) (1998) 93–116.

[27] E.A. Alkan, S. Goker, H. Sarigul, E. Yıldırım, Y.A. Udum, L. Toppare, The impact of [1,2,5]chalcogenazolo[3,4-f]-benzo[1,2,3]triazole structure on the optoelectronic properties of conjugated polymers, J. Polym. Sci. 58 (7) (2020) 956–968.

[28] A. Tang, W. Song, B.o. Xiao, J. Guo, J. Min, Z. Ge, J. Zhang, Z. Wei, E. Zhou, Benzotriazole-Based Acceptor and Donors, Coupled with Chlorination, Achieve a High VOC of 1.24 V and an Efficiency of 10.5% in Fullerene-Free Organic Solar Cells, Chem. Mater. 31 (11) (2019) 3941–3947.

[29] P.-I. Lee, S. Lien-Chung Hsu, J.F. Lee, H.-Y. Chuang, P. Lin, New conjugated copolymers based on benzo[1,2-b; 3,4-b′]dithiophene and derivatives of benzo[g] quinoxaline for bulk heterojunction solar cells, J. Polym. Sci., Part A: Polym. Chem. 49 (3) (2011) 662–670.

[30] M. Yasa, S. Surmeli, T. Depci, L. Toppare, S.O. Hacioglu, Synthesis of a Multifunctional Quinoxaline and Benzodithiophene Bearing Polymer and Its Electrochromic Device Applications, Macromol. Chem. Phys. 221 (6) (2020) 1900470, https://doi.org/10.1002/macp.v221.610.1002/macp.201900470.

[31] E.G. Cansu-Ergun, Chemical Insight Into Benzimidazole Containing Donor-Acceptor-Donor Type Π-Conjugated Polymers: Benzimidazole As An Acceptor, Polym. Rev. 58 (1) (2018) 42–62.

[32] J. Kuwabara, T. Yasuda, N. Takase, T. Kanbara, Effects of the Terminal Structure, Purity, and Molecular Weight of an Amorphous Conjugated Polymer on Its Photovoltaic Characteristics, ACS Appl. Mater. Interfaces 8 (3) (2016) 1752–1758.

[33] R. Acharya, S. Cekli, C.J. Zeman, R.M. Altamimi, K.S. Schanze, Effect of Selenium Substitution on Intersystem Crossing in π-Conjugated Donor–Acceptor–Donor Chromophores: The LUMO Matters the Most, J. Phys. Chem. Lett. 7 (4) (2016) 693–697.

[34] A. Punzi, E. Maiorano, F. Nicoletta, D. Blasi, A. Ardizzone, N. Ventosa, I. Ratera, J. Veciana, G.M. Farinola, 1,2,3-Triazole–Diketopyrrolopyrrole Derivatives with Tunable Solubility and Intermolecular Interactions, Eur. J. Org. Chem. 2016 (15) (2016) 2617–2627.

[35] Y. Gwon, S. Jo, H.-J. Lee, S.Y. Park, T.S. Lee, Synthesis of donor-acceptor-type conjugated polymer dots as organic photocatalysts for dye degradation and hydrogen evolution, Polymer 229 (2021), 124004.

[36] R.S. Kularatne, H.D. Magurudeniya, P. Sista, M.C. Biewer, M.C. Stefan, Donor–acceptor semiconducting polymers for organic solar cells, J. Polym. Sci., Part A: Polym. Chem. 51 (4) (2013) 743–768.

[37] F.V. Yaylali, H. Ozel, Y.A. Udum, L. Toppare, S. Soylemez, G. Gunbas, ProTOT: Synthesis of the missing member of the 3,4-chalcogen substituted bridged thiophenes and its utilization in donor-acceptor polymers, Polymer 212 (2021), 123076.

[38] F. Dumur, Recent advances on ferrocene-based photoinitiating systems, Eur. Polym. J. 147 (2021), 110328.

[39] G. March, T. Nguyen, B. Piro, Modified Electrodes Used for Electrochemical Detection of Metal Ions in Environmental Analysis, Biosensors 5 (2) (2015) 241–275.

[40] M.-A. Tehfe, F. Louradour, J. Lalevée, J.-P. Fouassier, Photopolymerization Reactions: On the Way to a Green and Sustainable Chemistry, Appl. Sci. 3 (2013) 490–514.

[41] S. Dadashi-Silab, S. Doran, Y. Yagci, Photoinduced Electron Transfer Reactions for Macromolecular Syntheses, Chem. Rev. 116 (17) (2016) 10212–10275.

[42] B. Dellago, A. Ricke, T. Geyer, R. Liska, S. Baudis, Photopolymerizable precursors for degradable biomaterials based on acetal moieties, Eur. Polym. J. 154 (2021), 110536.

[43] A.D. Tran, T. Koch, P. Knaack, R. Liska, Radical induced cationic frontal polymerization for preparation of epoxy composites, Compos. Part A: Appl. Sci. Manuf. 132 (2020) 105855, https://doi.org/10.1016/j.compositesa:2020.105855.

[44] S. Liu, Y. Zhang, K. Sun, B. Graff, P. Xiao, F. Dumur, J. Lalevée, Design of photoinitiating systems based on the chalcone-anthracene scaffold for LED cationic photopolymerization and application in 3D printing, Eur. Polym. J. 147 (2021), 110300.

[45] A. Cosola, M. Sangermano, D. Terenziani, R. Conti, M. Messori, H. Grützmacher, C. F. Pirri, A. Chiappone, DLP 3D – printing of shape memory polymers stabilized by thermoreversible hydrogen bonding interactions, Appl. Mater. Today 23 (2021), 101060.

[46] L. Pezzana, M. Sangermano, Fully biobased UV-cured thiol-ene coatings, Prog. Org. Coat. 157 (2021), 106295.

[47] Y. Yagci, W. Schnabel, New aspects on the photoinitiated free radical promoted cationic polymerization, Makromolekulare Chemie, Macromol. Symposia 60 (1) (1992) 133–143.

[48] Y. Yagci, S. Jockusch, N.J. Turro, Mechanism of Photoinduced Step Polymerization of Thiophene by Onium Salts: Reactions of Phenyliodinium and Diphenylsulfinium Radical Cations with Thiophene, Macromolecules 40 (13) (2007) 4481–4485.

[49] B. Aydogan, Y. Yagci, L. Toppare, S. Jockusch, N.J. Turro, Photoinduced Electron Transfer Reactions of Highly Conjugated Thiophenes for Initiation of Cationic Polymerization and Conjugated Polymer Formation, Macromolecules 45 (19) (2012) 7829–7834.

[50] T. Celiker, R. İsci, K. Kaya, T. Ozturk, Y. Yagci, Photoinduced step-growth polymerization of thieno[3,4-b] thiophene derivatives. The substitution effect on the reactivity and electrochemical properties, J. Polym. Sci. 58 (17) (2020) 2327–2334.

[51] E. Sari, G. Yilmaz, S. Koyuncu, Y. Yagci, Photoinduced Step-Growth Polymerization of N-Ethylcarbazole, J. Am. Chem. Soc. 140 (40) (2018) 12728–12731.

[52] K. Kaya, S. Koyuncu, Y. Yagci, Photoinduced synthesis of poly(N-ethylcarbazole) from phenacylium salt without conventional catalyst and/or monomer, Chem. Commun. 55 (77) (2019) 11531–11534.

[53] T. Celiker, K. Kaya, S. Koyuncu, Y. Yagci, Polypyrenes by Photoinduced Step-Growth Polymerization, Macromolecules 53 (14) (2020) 5787–5794.

[54] T. Celiker, A. Suerkan, S. Altinisik, M. Akgun, S. Koyuncu, Y. Yagci, Hollow microspherical carbazole-based conjugated polymers by photoinduced step-growth polymerization, Polym. Chem. 12 (32) (2021) 4654–4660.

[55] A. Suerkan, E.A. Alkan, K. Kaya, Y.A. Udum, L. Toppare, Y. Yagci, Highly conjugated visible and near-infrared light photoinitiating systems for radical and cationic polymerizations, Prog. Org. Coat. 154 (2021), 106189.